Food Research International 66 (2014) 78–85

Contents lists available at ScienceDirect

Food Research International

journal homepage: www.elsevier.com/locate/foodres

High throughput production of double emulsions using packed bed premix emulsification

Sami Sahin [a,*], Hassan Sawalha [b,1,*], Karin Schroën [a]

[a] Wageningen University, Food Process Engineering Group, Bornse Weilanden 9, 6708 WG Wageningen, The Netherlands
[b] An-Najah National University, Chemical Engineering Department, P.O. Box 7, Nablus, Palestine

ARTICLE INFO

Article history:
Received 28 May 2014
Accepted 24 August 2014
Available online 30 August 2014

Keywords:
Premix membrane emulsification
Double emulsion
Encapsulation
Packed bed
Droplet break-up

ABSTRACT

We explored the potential of packed bed premix emulsification for homogenizing coarse food grade W/O/W emulsions, prepared with sunflower oil. Using packed beds with different glass bead sizes (30–90 μm) at different applied pressures (200–600 kPa), emulsions with reasonably uniform droplet size (span ~ 0.75) were produced successfully at high fluxes (100–800 $m^3\ m^{-2}\ h^{-1}$). Sodium chloride was used as a release marker: after five homogenization cycles, the produced emulsions were found to retain almost all of their initial content (99%). As was previously found for single emulsions, the packed bed system proved to be effective in breaking up the W/O/W emulsion droplets, with droplet to pore size ratios as low as 0.3. Results were analysed through the pore Reynolds number, Re_p, which characterizes the flow inside the packed bed, and were related back to the droplet break-up mechanisms occurring. At high Re_p, droplet break-up was expected to be governed by shear forces while at low Re_p, there is a shift from shear based to spontaneous droplet break-up.

1. Introduction

Double emulsions (DEs) are emulsions of emulsions and if they can be prepared in sufficient quantity, which is far from trivial due to their inherent fragility, they possess great potential for application amongst others in food, pharmaceutics, cosmetics and chemicals (van der Graaf, Schroën, & Boom, 2005). For example, low calorie food products (de Cindio & Cacace, 1995; Garti, 1997; Lobato-Calleros, Rodriguez, Sandoval-Castilla, Vernon-Carter, & Alvarez-Ramirez, 2006), taste masking (Muschiolik, 2007; van der Graaf et al., 2005), encapsulation and controlled release of flavour and functional ingredients (Bonnet et al., 2009; Choi, Decker, & McClements, 2009; Garti, 1997; Muschiolik, 2007), or drug delivery systems (Hino, Yamamoto, Shimabayashi, Tanaka, & Tsujii, 2000; van der Graaf et al., 2005) may become a reality through application of double emulsions.

As mentioned, double emulsions are fragile and inherently difficult to make, which often results either in low encapsulation efficiency and/or fast release of the encapsulated component. Both aspects are used to characterize and compare preparation processes for double emulsions (van der Graaf et al., 2005). Controlling the stability and/or instability of DEs is important; on the one hand, the amount of encapsulated material should be as high as possible and the product should be stable on the shelf, while on the other hand, the DEs should become unstable upon experiencing a specific trigger. These are often contradictory demands, and many studies have addressed the challenges and possible strategies related to the stability of W/O/W emulsions, mostly through selection of the formulation and controlling droplet size (Bonnet et al., 2009; Bonnet et al., 2010; Bonnet et al., 2010; Garti, 1997; Muschiolik, 2007; Sapei, Naqvi, & Rousseau, 2012; Weiss & Muschiolik, 2007; Yafei, Tao, & Gang, 2006). The progress made in this field is encouraging (i.e., in relation to formulation parameter studies of DEs), although it also should be mentioned that clear guidelines that connect the various product (and process) parameters are not available, and we think that this is essential to make a product reproducibly. The interested reader is referred through to a recent review on double emulsions and the aspects that affect their stability (Muschiolik, 2007).

Clearly, the method of dispersion is of great importance, as it influences the initial encapsulation efficiency; however this aspect has received much less attention in literature. Using classic emulsification methods, only widely distributed large droplets can be produced at low-shear conditions, otherwise the internal phase is destroyed through the shearing action of the emulsification device, which results in low encapsulation efficiency (van der Graaf et al., 2005). For instance the encapsulation efficiency obtained with a laboratory mixer at high shear rate was 50–60% (Dickinson, Evison, & Owusu, 1991). Therefore,

* Corresponding authors. Tel.: +31 317 485411.
E-mail addresses: sami.sahin@wur.nl (S. Sahin), hassan.sawalha@gmail.com (H. Sawalha).
[1] Visiting researcher at the Food Process Engineering Group, Wageningen University, Wageningen, The Netherlands, where the work presented in this paper was conducted.

http://dx.doi.org/10.1016/j.foodres.2014.08.025
0963-9969/

production processes that allow adequate control over the preparation process and suppress release during the production have to be developed. There are already some examples of microchannel and membrane processes reported to yield encapsulation efficiencies higher than 90% (Shima et al., 2004; Sugiura et al., 2004).

For the production of single emulsions, techniques based on microstructured devices, such as membranes and microfluidic devices, are known to be much less energy intensive as classic emulsification technology (Gijsbertsen-Abrahamse, van der Padt, & Boom, 2004; Sugiura, Nakajima, Iwamoto, & Seki, 2001). In the preparation of single emulsions, microfluidic devices are known for their outstanding control over droplet size and size distribution. In this aspect, they clearly outperform membrane emulsification systems while they lag behind in terms of productivity (Anna, Bontoux, & Stone, 2003; Garstecki, Stone, & Whitesides, 2005; Link, Anna, Weitz, & Stone, 2004; Maan, Schroën, & Boom, 2013; Steegmans, Schroën, & Boom, 2009; Sugiura, Nakajima, & Seki, 2002; van Dijke, de Ruiter, Schroën, & Boom, 2010; Vladisavljević, Kobayashi, & Nakajima, 2008). In some cases it even has been reported that microstructured devices can be used for double emulsion preparation (Muschiolik, 2007; Nisisako, 2008; Sugiura et al., 2004; van Dijke, Schroën, van der Padt, & Boom, 2010; Vladisavljević, Shimizu, & Nakashima, 2004; Zhao, 2013).

When using microstructured devices, emulsification is mostly carried out starting from two phases that are dispersed into each other as is for example the case in cross-flow membrane emulsification (ME), but alternatively also a coarse emulsion may be used as a starting point, as is the case in premix membrane emulsification. Compared to cross-flow ME, premix ME allows higher dispersed phase fractions at high production rates at the expense of a lower but still reasonable monodispersity (Nazir, Schroën, & Boom, 2010); whether that also holds for double emulsion preparation with sieve-supported packed beds is one of the questions covered by this paper.

The regular membranes used in premix membrane emulsification, such as Shirasu porous glass (SPG) and polymeric membranes are sensitive to depth fouling and the fouled pores are not accessible to cleaning agents, which limits the use of these systems (Nazir, Schroën, & Boom, 2013; van der Zwan, Schroën, & Boom, 2008). It is also expected that the internal phase of the double emulsions interacts with the membrane, and that will result in untimely release of the encapsulated component. Clearly interactions with the membrane need to be minimised, and this makes the recently introduced metal sieves with straight-through pores an interesting alternative, also because they allow operation at much higher fluxes as reported for regular membranes when used for single emulsion production (Nazir, Schroën, & Boom, 2011). Likewise, using a supported packed bed of micron size glass beads, acting as a dynamic membrane, allows for the system to be disintegrated, cleaned and reused afterwards (van der Zwan et al., 2008). For O/W emulsification, both metal sieves and packed bed system were reported to have at least an order of magnitude higher fluxes than often reported for SPG membranes, while the packed bed system gave better monodispersity (span = 0.75) than metal sieves alone (span = 1.0–1.4). The significant difference in droplet size distribution was suggested to be due to the change in droplet break-up mechanism, going from inertia to constriction for sieves and packed beds respectively (Nazir, Boom, & Schroën, 2013; Nazir, Schroën, & Boom, 2013).

In this paper, we explore the potential of packed bed systems for the preparation of W/O/W double emulsions, and compare the obtained results with those of other premix emulsification studies. We investigated various parameters, such as applied pressure, bed structure, and number of homogenization cycles, and report droplet size and distribution, and fluxes. Besides we relate the results back to droplet break-up mechanism through analysis of the pore Reynolds number (as defined in Eq. (9)). Encapsulation stability and release characteristics of the emulsions during storage are not the major scope of this work, so this aspect will only be discussed briefly.

2. Experimental

2.1. Materials

MilliQ ultra-pure water was used for the preparation of the aqueous phases. Sunflower oil was purchased from a local supermarket (Wageningen, The Netherlands). Sodium chloride (NaCl) (Merck KGaA, Darmstadt, Germany) was used as a release marker in the inner aqueous phase. Glucose monohydrate (Merck, Darmstadt, Germany) was incorporated in the outer aqueous phase to counterbalance the osmotic pressure exerted by NaCl in the inner aqueous phase. Tween-20 (Sigma, USA) and polyglycerol polyricinoleate (PGPR) (Givaudan, Vernier, Switzerland) were used as water and oil soluble emulsifiers, respectively, as described in the next section. All components are food grade.

2.2. Coarse W/O/W preparation

For each experiment, a 300 mL batch of W/O/W emulsion was prepared at room temperature (23–27 °C) in two steps. For the preparation of the primary W/O emulsion, 1 M NaCl solution was dispersed at 25% (v/v) into sunflower oil containing 5% PGPR using an Ultra-Turrax homogenizer (IKA® T-18 basic, Staufen, Germany) at 11,000 rpm for 6 min. The typical Sauter mean diameter, d_{32}, of the inner water droplets was 0.22 ± 0.01 μm with a span of 2 ± 0.1; please note that this emulsion could be reproducibly obtained. The secondary emulsion (W/O/W) was prepared by gradually adding 15 mL of the primary emulsion (W/O) to the outer aqueous phase (285 mL of 2 M glucose monohydrate solution containing 0.5% v/v Tween-20) under mixing on a magnetic stirrer (IKA® KMO 2 basic, Staufen, Germany) at 700 rpm for 16 min. The coarse double emulsion had typical Sauter mean diameters, d_{32}, of 45 μm with an average span of 4.

The Sauter mean diameter, d_{32}, is defined as follows:

$$d_{32} = \frac{6}{S_v} = \left(\sum_{i=1}^{n_s} \frac{v_i}{d_i}\right)^{-1} \quad (1)$$

where S_v is the droplet surface area per unit volume, v_i is the volume fraction of droplets in the i^{th} size class of the discretized distribution, d_i is the mean droplet diameter in that class, and n_s is the number of size classes.

The span, indicating the uniformity of the droplet size distribution, is defined as:

$$\delta = \frac{d_{90} - d_{10}}{d_{50}} \quad (2)$$

where d_x is the droplet diameter corresponding to x% volume on a cumulative droplet size distribution curve.

2.3. Experimental setup and emulsification procedure

The premix emulsification setup is schematically presented in Fig. 1. The pressure vessel was connected to a nitrogen supply and the packed bed module. The packed bed module consisted of a column made of polymethyl methacrylate (built by the mechanical workshop of Wageningen University), at the bottom of which a nickel sieve (described in Section 2.4) was placed between two rubber O-rings. The nickel sieve served as a support to the layer of hydrophilic glass beads placed on it.

The prepared 300 mL premix W/O/W was placed in the pressure vessel and the vessel was pressurized through the nitrogen supply; typical applied pressures were 200–600 kPa. The emulsification was started by opening the outlet valve of the packed bed column and the homogenized emulsion was collected in a flask placed on an electrical balance connected to a computer through which the increase in mass per

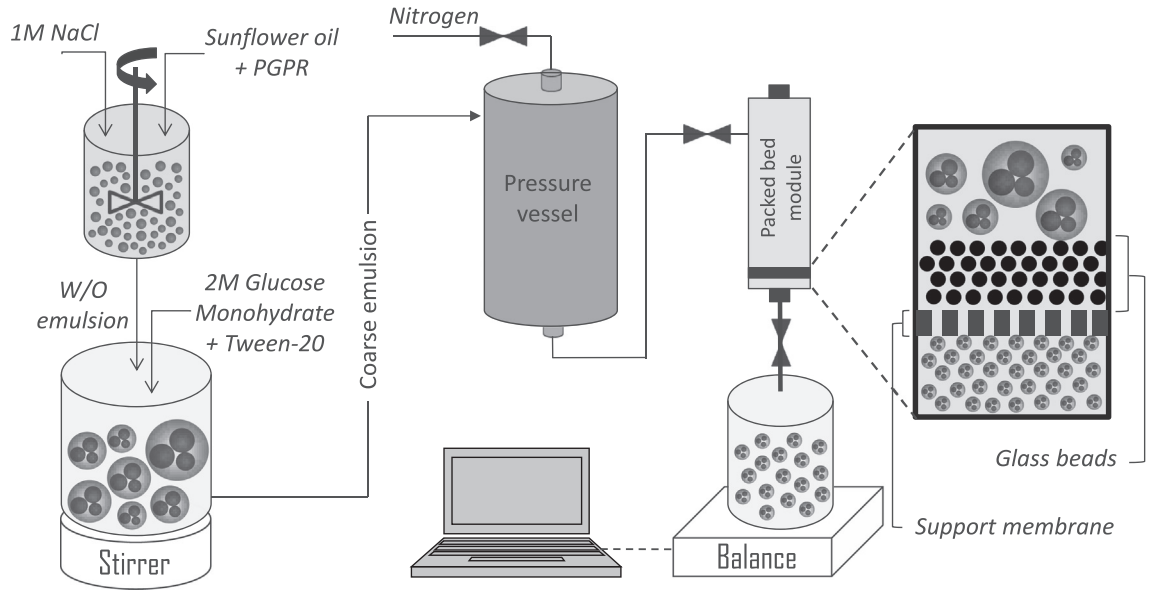

Fig. 1. Schematic representation of the experimental set-up and emulsification procedure.

second was recorded. The flux across the packed bed, J, was calculated from the mass flow rate ϕ_m, through the following formula:

$$J = \frac{\phi_m}{\rho_e A} \tag{3}$$

where ρ_e is the emulsion density and A is the effective surface area of the packed bed.

The homogenization cycle was repeated five times and samples from each pass were collected for sizing with the Mastersizer as described in Section 2.6. The oil droplet size of the obtained emulsions was very reproducible (<5% error), as was the case for single emulsions. This is illustrated in Fig. 2 with two examples of size distributions obtained for duplicated experiments.

2.4. Nickel sieve

The nickel sieves used as a support were obtained from Veco B.V., Eerbeek, The Netherlands. The specifications and SEM images of the sieve used are given in Table 1. In our experiments the sieves were placed in the column in such a way that their front side was facing the glass beads, although it should be mentioned that placing the sieve the other way around had no influence on the results.

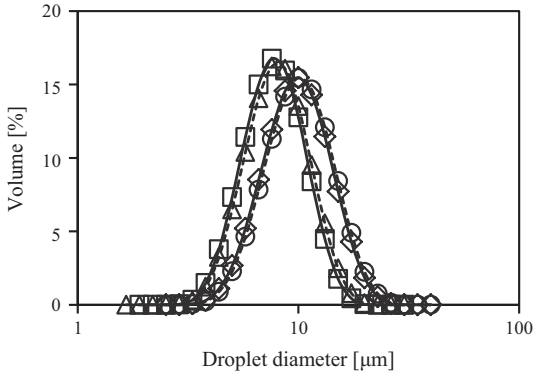

Fig. 2. The size distribution of oil droplets containing inner water droplets for two duplicate experiments conducted at 400 kPa and at a bed height, H_{bed}, of 2 mm. Two different bead sizes, d_b, were used: (□) and (Δ) $d_b = 55$ μm; (○) and (◊) $d_b = 30$ μm.

2.5. Packed bed and characterisation of the flow

The packed bed module was prepared by packing glass beads of different sizes on the support sieve. A close-up of the packed bed is sketched at the right side of Fig. 1, and the characteristics of the glass beads used and resulting packed bed are given in Table 2. Five different bead size fractions were obtained by sieving from a stock of glass beads (100HFL, Pneumix SMG-AF) with a wide size distribution (30–200 μm) as described in Nazir, Boom, and Schroën (2013).

The porosity of the packed bed, ε, was calculated as:

$$\varepsilon = 1 - \frac{\rho_b}{\rho_p} \tag{4}$$

where ρ_b and ρ_p are the measured bulk and particle density of the beads.

To determine the structural properties of the packed bed such as pore diameter and bed tortuosity, the adopted capillary model for fixed beds proposed by Comiti and Renaud (1989) was used. Pore diameter, d_p, was defined as follows:

$$d_p = \frac{4\varepsilon}{A_{vd}(1-\varepsilon)} \tag{5}$$

where A_{vd} is the specific surface area, which is the ratio of a particle's surface area to its volume. For a spherical particle, glass bead in this case:

$$A_{vd} = \frac{6}{d_b} \tag{6}$$

Table 1
Specifications of the nickel sieve used together with its front and back side SEM images.

Sieve specifications	Front view	Back view
Pore size: 11.6 × 331 μm Thickness: 350 μm Porosity: 3.95% Effective surface area: 1.43 cm^2	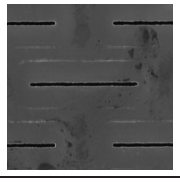	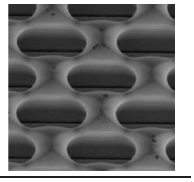

Table 2
Characteristics of the glass beads and resulting packed bed.

Bead specifications		Bed properties	
Diameter, d_b [μm]	Span, δ [−]	Pore diameter, d_p [μm]	Porosity, ε [−]
30	1.14	13.33	0.4
55	0.82	24.44	0.4
65	0.65	28.89	0.4
78	0.65	33.33	0.4
90	0.64	40.00	0.4

The bed tortuosity, ξ, was calculated as:

$$\xi = 1 + q \ln(1/\varepsilon) \tag{7}$$

where q is 0.41 for tightly packed spheres.

The average pore velocity, ν_p, was calculated as:

$$\nu_p = \frac{\nu_o \xi}{\varepsilon} \tag{8}$$

where ν_o is the superficial velocity equal to flux across the packed bed, J. The flow inside the packed bed is characterized using the pore Reynolds number, Re_p, which is defined as:

$$Re_p = \frac{\rho_e \nu_p d_p}{\eta_e} \tag{9}$$

where η_e is the emulsion viscosity.

2.6. Characterization of W/O/W emulsions

The size (distribution) of the oil droplets in all W/O/W emulsions was determined with a laser diffraction particle size analyser (Mastersizer 2000, Malvern Instruments Ltd., UK). Although the oil droplets contained small inner water droplets which may induce inhomogeneity in laser diffraction signal, the dispersed phase was assumed to be pure sunflower oil. For a random selection of samples, it was checked whether the measured droplet size values were in agreement with microscopic observations, and this was always the case. The average of three readings from the Mastersizer was taken for droplet size and droplet size distribution (span).

2.7. Encapsulation efficiency

Encapsulation efficiency (EE %) was expressed as the percentage of NaCl retained in the oil droplets relative to the total amount added. Both for freshly prepared and stored W/O/W samples, encapsulation efficiency was determined by quantifying the amount of NaCl released through conductivity measurement (SevenMulti meter, Mettler Toledo International Inc., USA) and using a calibration curve. The encapsulation efficiency was calculated as follows:

$$\text{EE } \% = \left(\frac{C_{total} - C_{w2}}{C_{total}}\right) \times 100 \tag{10}$$

where C_{w2} is the concentration of NaCl released into the outer aqueous phase and C_{total} is the concentration of NaCl in case all NaCl in the inner aqueous phase were released into the outer aqueous phase.

3. Results and discussion

For the preparation of single emulsions using packed bed premix emulsification, Nazir and co-workers established scaling relations taking into account process parameters such as bead size, bed height and applied pressure (Nazir, Boom, & Schroën, 2013). The dynamics of double emulsion droplets and their break-up mechanism are not well understood (Chen, Liu, & Shi, 2013), therefore it is expected that the scaling relations derived by Nazir, Boom, and Schroën (2013) may not hold. In the present work, we first have briefly discussed the effects of some of the process parameters individually, and compiled the results into a dimensionless plot from which conclusions regarding droplet break-up mechanisms were made. Besides, the effect of process settings on the encapsulation efficiency was investigated.

3.1. Applied pressure

First the effect of applied pressure on flux was investigated for a bed with 65 μm glass beads of 2 mm height (see Fig. 3). The flux increased fairly linearly with pressure especially at the 3rd and 5th passes, which is as expected for a single phase system. The actual flux values were in agreement with those found for single emulsions (Nazir, Boom, & Schroën, 2013). The linear behaviour indicates that in general the double emulsions behaved as one liquid, and that the droplets did not accumulate before or while passing the bed. Possibly, the data point measured at 500 kPa for the first pass was an exception; for these settings we repeatedly found that the flux increased less than expected, and this could indicate that emulsion droplets (slightly) accumulated in or before the bed. This could also be the case for other passes for which the flux values were slightly lower as for the first pass; there were simply more droplets present due to the refinement that took place, and those may have increased the effective viscosity in the pores and the packed bed leading to slightly lower fluxes.

When comparing the obtained fluxes with literature, it is clear that they are much higher than the highest reported fluxes (at 150 kPa) for the production of W/O/W by premix membrane emulsification (ME) with SPG membranes (10.7 μm mean pore diameter, porosity of 55.2% and tortuosity of 1.3) (Vladisavljević, Shimizu, & Nakashima, 2006; Vladisavljević et al., 2004), while there is room for further improvement by increasing the pressure in the current investigation. On the other hand, the fluxes obtained are a factor of 3 lower than those reported by Nazir, Boom, and Schroën (2013) for single emulsions using packed bed systems. This is because the double emulsion had 3.6 times higher apparent viscosity (3.6 mPa s) than single emulsions (i.e., flux scales reciprocally with viscosity).

In Fig. 4, the size of the droplets relative to the calculated pore size, and the span of the obtained droplet size distribution are shown. The size of the droplets was always smaller than the pore size, and this indicates that the bed was rather effective in droplet break-up, as was previously reported for single emulsions. In SPG cross-flow membrane emulsification, the size of the droplets that are generated is always 2–10 times the pore size (Charcosset, Limayem, & Fessi, 2004); in spontaneous emulsification microfluidics, the droplet size is 3–6 times that of the smallest dimension of the droplet formation unit (Kobayashi, Mukataka, & Nakajima, 2004; Sugiura, Nakajima, Kumazawa,

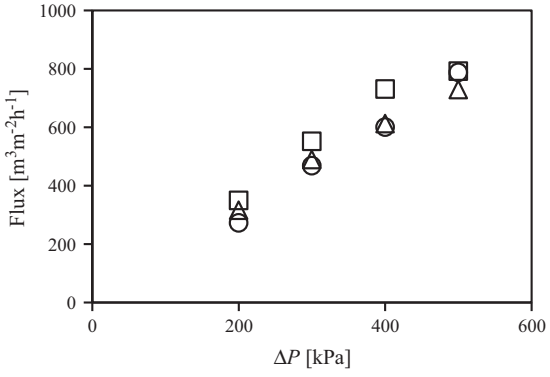

Fig. 3. Transmembrane flux obtained through the 65 μm glass beads at a bed height, H_{bed}, of 2 mm as a function of applied pressure, ΔP: (□) 1st pass, (Δ) 3rd pass, (○) 5th pass.

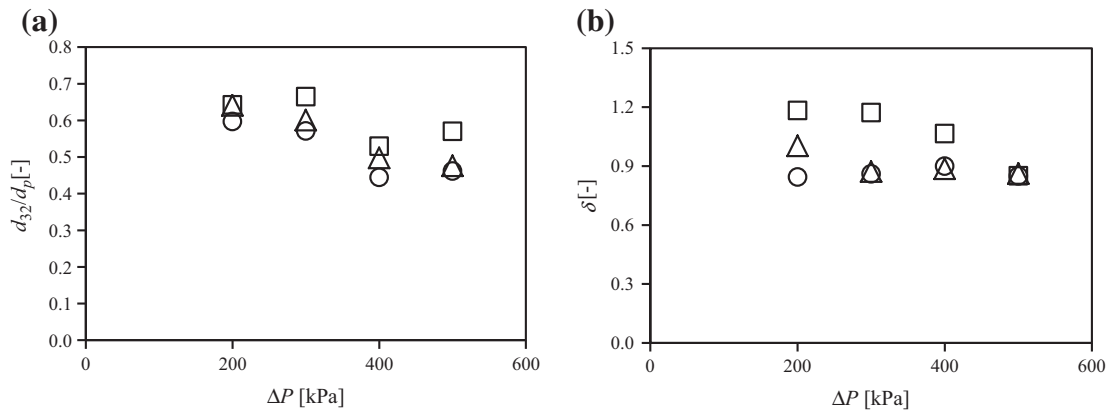

Fig. 4. (a) Dimensionless droplet diameter, d_{32}/d_p, and (b) droplet span, δ, obtained through the 65 μm glass beads at a bed height, H_{bed}, of 2 mm as a function of applied pressure, ΔP: (□) 1st pass, (Δ) 3rd pass, (○) 5th pass.

Iwamoto, & Seki, 2002; van Dijke, de Ruiter, Schroën, & Boom, 2010; van Dijke, Schroën, van der Padt, & Boom, 2010), therewith indicating the differences between the methods.

As expected, a higher size reduction was achieved at higher applied pressure, which is associated with the higher shear stresses inside the pore labyrinth as a result of increased flow velocity. Possibly, also the number of active pores increased, but that can only explain the observation if the velocity in the pores was also higher at high pressure. Given the size of the pores it is expected that they were all active, and that increasing the pressure mainly influenced the average velocity in the pores, not so much the amount of active pores. At all applied pressures, the largest average droplet size reduction was found after the first pass after which only a slight reduction was observed.

The droplet size distribution after the first pass was wider at low applied pressures compared to the higher ones, but the eventually obtained span was independent of the applied pressure (Fig. 4b). This is attributed to the higher pore velocity at higher pressures leading to more efficient droplet break-up, which has led to the final span being reached after less passes.

3.2. Droplet break-up mechanism

In premix emulsification, droplet break-up can be governed by localized shear forces (see also previous section), interfacial tension effects and steric hindrance between droplets (van der Zwan, Schroën, van Dijke, & Boom, 2006). While under different conditions, one mechanism may dominate the droplet break-up, all three are expected to operate simultaneously. The interested reader is referred to a recent review on premix emulsification by Nazir et al. (2010) for more information.

To distinguish between different droplet break-up mechanisms, we performed a series of experiments, systematically varying the bead size, bed height and applied pressure as shown in Table 3, leading to a wide range of process conditions. In Fig. 5a, the final droplet to pore size ratios obtained after the fifth pass are plotted against the corresponding pore Reynolds number which characterizes the flow inside the packed bed as discussed in Section 2.5.

Table 3
Process conditions for the experiments plotted in Fig. 5 with corresponding symbols.

Experiment	Bead size [μm]	Applied pressure [kPa]	Bed height [mm]
(○)	30, 55, 65, 78, 90	400	2
(◊)	65	400	2, 5, 20, 40
(□)	65	200, 300, 400, 500	2
(▲)	55	200, 400, 600	2
(Δ)	30	200, 400, 600	2

In Fig. 5a, two regions can be distinguished, one at high Re_p at which the size reductions coincided regardless of the bead size and bed height used, and one at low Re_p, in which the size reductions did not coincide. This transition between the two regions took place between Re_p 1 and 2. In the high Re_p region, it is expected that shear forces dominated droplet break-up, as was also found in the work of Nazir, Boom, and Schroën (2013) for single emulsions. At low Re_p the obtained values were scattered, and they were even more scattered as found for single emulsions. We expect that part of the explanation for this lies in a transition from shear based to spontaneous droplet break-up with, in the latter case, small beads being more efficient in droplet break-up (Nazir, Boom, & Schroën, 2013). It should be mentioned that the effects are not completely in line with what was observed for single emulsions; the highest and lowest size reductions were achieved with 55 and 30 μm glass beads, respectively, and an intermediate reduction was achieved with 65 μm beads.

In an attempt to explain this, we analysed the results of similar premix emulsification studies (Nazir, Boom, & Schroën, 2013; Vladisavljević et al., 2006), and compared them with our findings. Nazir, Boom, and Schroën (2013) found that a packed bed of smaller beads was more effective in droplet break-up in the constriction dominated spontaneous emulsification region (at low Re_p) for the homogenization of O/W emulsions, for which they used 55 and 78 μm glass beads. At the low Re_p region in the current study, we also observed a similar trend in droplet size reduction with bead size used. However, the smallest beads (30 μm), being less efficient in size reduction, seemed to be the exception to the rule. The droplet size decreased considerably upon increasing the applied pressure, and this could indicate that at low pressure the internal droplets interact with the glass beads, possibly leading to congestion of droplets and even re-coalescence inside the bed, and less efficient break-up. This explanation could be in line with the findings of Vladisavljević et al. (2006) for premix membrane emulsification using SPG membranes with various pore sizes (5.4 to 20.3 μm) that more homogenization cycles are needed for smaller pores to attain a similar droplet size reduction.

In all cases, the droplet size was smaller than the pore size, with a lowest droplet to pore size ratio of around 0.3 both at low and high pore Reynolds numbers. A similar overall size reduction was also reported by Nazir and co-workers for the preparation of O/W emulsions using packed bed systems, although it should be mentioned that the highest pore Reynolds numbers given in their study were typically a factor of 4 higher as reached in the current study due to viscosity differences (Nazir, Boom, & Schroën, 2013). In some cases, the droplet to pore size ratios obtained in our work were significantly higher than those reported for single emulsions. This is attributed to the deformation resistance of highly viscous dispersed phase (W/O) in our system (Chen et al., 2013), which has led to less effective droplet break-up.

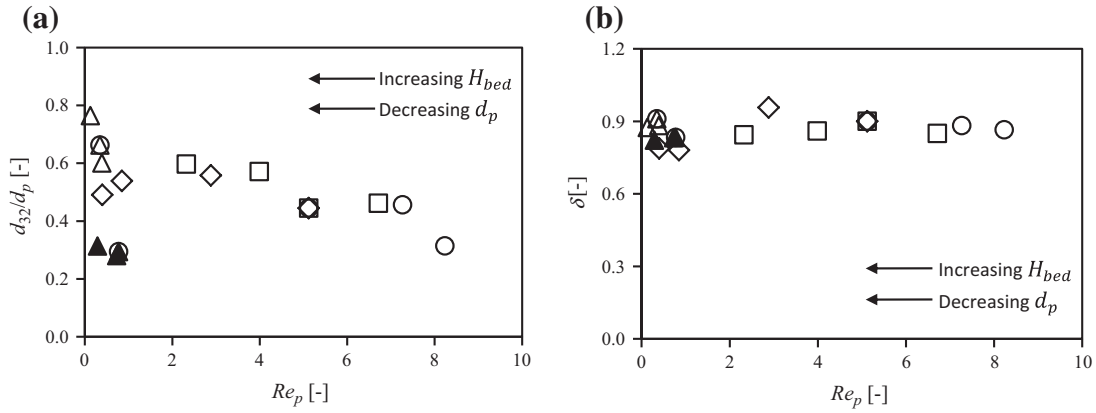

Fig. 5. (a) Dimensionless droplet diameter, d_{32}/d_p, and (b) droplet span, δ, as a function of the pore Reynolds number, Re_p. In both figures, ΔP varied (□) for the 65 μm beads, (▲) for the 55 μm beads, and (Δ) for the 30 μm beads; (○) pore size, d_p, varied through bead size, d_b; (◊) bed height, H_{bed}, varied from 2 to 40 mm for the 65 μm beads.

Table 4
Encapsulation efficiencies immediately after the 5th pass at different process conditions.

Bead size [μm]	Bed height [mm]	Applied pressure [kPa]	Encapsulation Efficiency (%)	Bead size [μm]	Bed height [mm]	Applied pressure [kPa]	Encapsulation efficiency (%)
90	2	400	>99	65	40	400	>98
78	2	400	>99	55	2	200	>97
65	2	200	>99	55	2	400	>95
65	2	300	>99	55	2	600	>95
65	2	400	>99	30	2	200	>94
65	2	500	>99	30	2	400	>94[a]
65	5	400	>99	30	2	400	>94[a]
65	20	400	>99	30	2	600	>91

[a] Duplicate experiments.

Compared to many other premix membrane emulsification studies focused on double emulsions, the size reductions we obtained are at the lower end of the reported range of 0.2–3.5 (Shima et al., 2004; Surh, Vladisavljević, Mun, & McClements, 2007; Vladisavljević et al., 2004; Vladisavljević et al., 2006), which shows the effectiveness of the packed bed system in breaking up the double emulsion droplets.

Interestingly enough, in spite of all the mechanisms happening, the span values were reasonably low and in close proximity, which suggests that under all considered conditions, also the largest droplets in the starter emulsion were effectively reduced relative to the pore size used (Fig. 5b). This can partly be explained by the high viscosity ratio we used, for which Nazir, Boom, and Schroën (2014) also showed that in general droplet size distribution is narrower compared to those obtained at lower viscosity ratios.

3.3. Encapsulation efficiency

Besides appreciable size reductions, premix membrane emulsification of W/O/W emulsions with packed bed also yielded high encapsulation efficiencies. Table 4 shows the encapsulation efficiencies of double emulsions homogenized by passing five times through packed beds at various process conditions. Irrespective of the process conditions, double emulsion droplets were successfully homogenized, while retaining high percentages of their content.

Experiments conducted with larger beads (65, 78 and 90 μm) resulted in encapsulation efficiencies greater than 98%. On the other hand, in experiments with 30 and 55 μm beads, more of the encapsulated substance was released during homogenization (and this could also hint at interactions with the beads), however the encapsulation efficiencies were still above 90%. Fig. 6 shows the droplet size distribution of emulsions from two experiments right after preparation and after 1 day storage at room temperature. Despite the release occurring during storage, the droplet size distributions remained unchanged. As mentioned, the mechanism of release is outside the scope of the current study, but experimental results suggest that the release was diffusion controlled since the oil droplet size distribution was constant during storage, and the inner water droplets were clearly noticed in microscopy. In conclusion, the results showed that packed bed premix emulsification is a

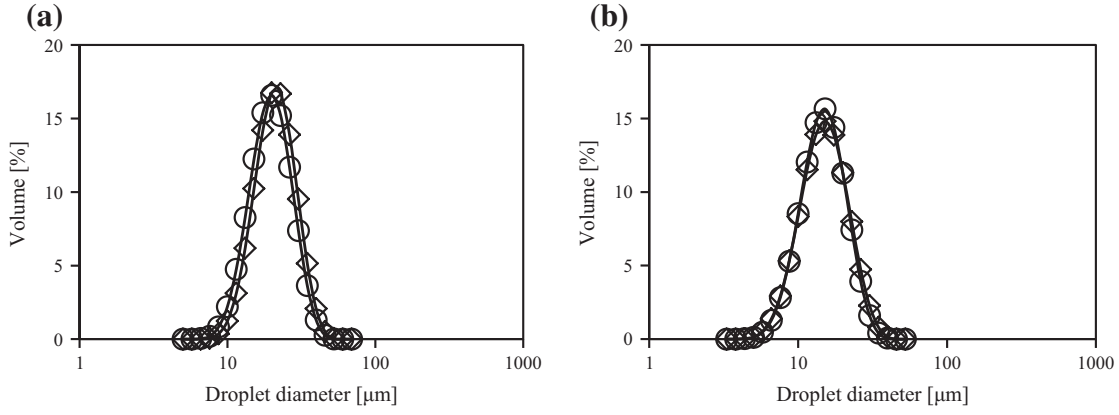

Fig. 6. Droplet size distribution of double emulsions: (○) 5th pass freshly prepared and (◊) 5th pass after 1 day storage at room temperature (23–27 °C). Processing parameters at which emulsions prepared were: (a) $d_b = 65$ μm, $H_{bed} = 2$ mm, $\Delta P = 200$ kPa, (b) $d_b = 65$ μm, $H_{bed} = 2$ mm, $\Delta P = 400$ kPa.

gentle technique capable of homogenizing W/O/W double emulsions without releasing the inner droplets.

4. Conclusion

Results show that a packed bed premix emulsification system is well-suited for the preparation of W/O/W emulsions. Along with the high throughput, the process allows high encapsulation efficiency and provides reasonably narrow droplet size distribution. Droplet size reductions achieved are comparable to those reported for single emulsions. Consistency of the experimental results indicates the robustness of the process.

Considering the above mentioned features and adding scalability, ease of operation, and cleanability of the system, this method can meet many of the industrial demands for large scale production of (double) emulsions.

Nomenclature

d_{32}	Sauter mean droplet diameter, see also Eq. (1) [m]
S_v	droplet surface area per unit volume [m^{-1}]
v_i	volume fraction of droplets in the i^{th} size class [dimensionless]
d_i	mean droplet diameter in the i^{th} size class [m]
n_s	number of size classes [dimensionless]
d_x	droplet diameter corresponding to x% volume on a cumulative droplet size distribution curve [m]
J	flux [$m^3\ m^{-2}\ s^{-1} = m\ s^{-1}$]
A	effective surface area of packed bed [m^2]
H_{bed}	packed bed height [m]
d_b	glass bead diameter [m]
d_p	pore diameter [m]
A_{vd}	specific surface area [$m^2\ m^{-3}$]
q	constant in Eq. (7) [dimensionless]
v_o	superficial velocity [$m\ s^{-1}$]
v_p	pore velocity [$m\ s^{-1}$]
Re_p	pore Reynolds number [dimensionless]
C_{w2}	concentration of released NaCl [$mol\ L^{-1}$]
C_{total}	concentration of NaCl if all released [$mol\ L^{-1}$]

Greek letters

ΔP	transmembrane pressure [Pa]
ρ_e	emulsion density [$kg\ m^{-3}$]
ϕ_m	mass flow rate [$kg\ s^{-1}$]
ε	porosity [dimensionless]
ξ	bed tortuosity [dimensionless]
ρ_b	bulk density [$kg\ m^{-3}$]
ρ_p	particle density [$kg\ m^{-3}$]
η_e	emulsion viscosity [Pa s]
δ	droplet span [dimensionless]

Acknowledgements

This work is supported by NanoNextNL, a micro and nanotechnology consortium of the Government of The Netherlands and 130 partners.

References

Anna, S. L., Bontoux, N., & Stone, H. A. (2003). Formation of dispersions using "flow focusing" in microchannels. *Applied Physics Letters*, *82*(3), 364–366.

Bonnet, M., Cansell, M., Berkaoui, A., Ropers, M. H., Anton, M., & Leal-Calderon, F. (2009). Release rate profiles of magnesium from multiple W/O/W emulsions. *Food Hydrocolloids*, *23*(1), 92–101.

Bonnet, M., Cansell, M., Placin, F., David-Briand, E., Anton, M., & Leal-Calderon, F. (2010). Influence of ionic complexation on release rate profiles from multiple water-in-oil-in-water (W/O/W) emulsions. *Journal of Agricultural and Food Chemistry*, *58*(13), 7762–7769.

Bonnet, M., Cansell, M., Placin, F., Monteil, J., Anton, M., & Leal-Calderon, F. (2010). Influence of the oil globule fraction on the release rate profiles from multiple W/O/W emulsions. *Colloids and Surfaces B: Biointerfaces*, *78*(1), 44–52.

Charcosset, C., Limayem, I., & Fessi, H. (2004). The membrane emulsification process—A review. *Journal of Chemical Technology and Biotechnology*, *79*(3), 209–218.

Chen, Y., Liu, X., & Shi, M. (2013). Hydrodynamics of double emulsion droplet in shear flow. *Applied Physics Letters*, *102*(5), 051609.

Choi, S. J., Decker, E. A., & McClements, D. J. (2009). Impact of iron encapsulation within the interior aqueous phase of water-in-oil-in-water emulsions on lipid oxidation. *Food Chemistry*, *116*(1), 271–276.

Comiti, J., & Renaud, M. (1989). A new model for determining mean structure parameters of fixed beds from pressure drop measurements: application to beds packed with parallelepipedal particles. *Chemical Engineering Science*, *44*(7), 1539–1545.

de Cindio, B., & Cacace, D. (1995). Formulation and rheological characterization of reduced-calorie food emulsions. *International Journal of Food Science & Technology*, *30*(4), 505–514.

Dickinson, E., Evison, J., & Owusu, R. K. (1991). Preparation of fine protein-stabilized water-in-oil-in-water emulsions. *Food Hydrocolloids*, *5*(5), 481–485.

Garstecki, P., Stone, H. A., & Whitesides, G. M. (2005). Mechanism for flow-rate controlled breakup in confined geometries: A route to monodisperse emulsions. *Physical Review Letters*, *94*(16), 164501–1645014.

Garti, N. (1997). Progress in stabilization and transport phenomena of double emulsions in food applications. *LWT — Food Science and Technology*, *30*(3), 222–235.

Gijsbertsen-Abrahamse, A. J., van der Padt, A., & Boom, R. M. (2004). Status of cross-flow membrane emulsification and outlook for industrial application. *Journal of Membrane Science*, *230*(1–2), 149–159.

Hino, T., Yamamoto, A., Shimabayashi, S., Tanaka, M., & Tsujii, D. (2000). Drug release from w/o/w emulsions prepared with different chitosan salts and concomitant creaming up. *Journal of Controlled Release*, *69*(3), 413–419.

Kobayashi, I., Mukataka, S., & Nakajima, M. (2004). CFD simulation and analysis of emulsion droplet formation from straight-through microchannels. *Langmuir*, *20*(22), 9868–9877.

Link, D. R., Anna, S. L., Weitz, D. A., & Stone, H. A. (2004). Geometrically mediated breakup of drops in microfluidic devices. *Physical Review Letters*, *92*(5), 0545031–0545034.

Lobato-Calleros, C., Rodriguez, E., Sandoval-Castilla, O., Vernon-Carter, E. J., & Alvarez-Ramirez, J. (2006). Reduced-fat white fresh cheese-like products obtained from $W_1/O/W_2$ multiple emulsions: Viscoelastic and high-resolution image analyses. *Food Research International*, *39*(6), 678–685.

Maan, A. A., Schroën, K., & Boom, R. (2013). Monodispersed water-in-oil emulsions prepared with semi-metal microfluidic EDGE systems. *Microfluidics and Nanofluidics*, *14*(1–2), 187–196.

Muschiolik, G. (2007). Multiple emulsions for food use. *Current Opinion in Colloid & Interface Science*, *12*(4–5), 213–220.

Nazir, A., Boom, R. M., & Schroën, K. (2013). Droplet break-up mechanism in premix emulsification using packed beds. *Chemical Engineering Science*, *92*, 190–197.

Nazir, A., Boom, R. M., & Schroën, K. (2014). Influence of the emulsion formulation in premix emulsification using packed beds. *Chemical Engineering Science*, *116*, 547–557.

Nazir, A., Schroën, K., & Boom, R. (2010). Premix emulsification: A review. *Journal of Membrane Science*, *362*(1–2), 1–11.

Nazir, A., Schroën, K., & Boom, R. (2011). High-throughput premix membrane emulsification using nickel sieves having straight-through pores. *Journal of Membrane Science*, *383*(1–2), 116–123.

Nazir, A., Schroën, K., & Boom, R. (2013). The effect of pore geometry on premix membrane emulsification using nickel sieves having uniform pores. *Chemical Engineering Science*, *93*, 173–180.

Nisisako, T. (2008). Microstructured devices for preparing controlled multiple emulsions. *Chemical Engineering Technology*, *31*(8), 1091–1098.

Sapei, L., Naqvi, M.A., & Rousseau, D. (2012). Stability and release properties of double emulsions for food applications. *Food Hydrocolloids*, *27*(2), 316–323.

Shima, M., Kobayashi, Y., Fujii, T., Tanaka, M., Kimura, Y., Adachi, S., et al. (2004). Preparation of fine W/O/W emulsion through membrane filtration of coarse W/O/W emulsion and disappearance of the inclusion of outer phase solution. *Food Hydrocolloids*, *18*(1), 61–70.

Steegmans, M. L. J., Schroën, K. G. P. H., & Boom, R. M. (2009). Characterization of emulsification at flat microchannel Y junctions. *Langmuir*, *25*(6), 3396–3401.

Sugiura, S., Nakajima, M., Iwamoto, S., & Seki, M. (2001). Interfacial tension driven monodispersed droplet formation from microfabricated channel array. *Langmuir*, *17*(18), 5562–5566.

Sugiura, S., Nakajima, M., Kumazawa, N., Iwamoto, S., & Seki, M. (2002). Characterization of spontaneous transformation-based droplet formation during microchannel emulsification. *The Journal of Physical Chemistry B*, *106*(36), 9405–9409.

Sugiura, S., Nakajima, M., & Seki, M. (2002). Preparation of monodispersed emulsion with large droplets using microchannel emulsification. *Journal of the American Oil Chemists' Society*, *79*(5), 515–519.

Sugiura, S., Nakajima, M., Yamamoto, K., Iwamoto, S., Oda, T., Satake, M., et al. (2004). Preparation characteristics of water-in-oil-in-water multiple emulsions using microchannel emulsification. *Journal of Colloid and Interface Science*, *270*(1), 221–228.

Surh, J., Vladisavljević, G. T., Mun, S., & McClements, D. J. (2007). Preparation and characterization of water/oil and water/oil/water emulsions containing biopolymer-gelled water droplets. *Journal of Agricultural and Food Chemistry*, *55*(1), 175–184.

van der Graaf, S., Schroën, C. G. P. H., & Boom, R. M. (2005). Preparation of double emulsions by membrane emulsification—A review. *Journal of Membrane Science*, *251*(1–2), 7–15.

van der Zwan, E. A., Schroën, C. G. P. H., & Boom, R. M. (2008). Premix membrane emulsification by using a packed layer of glass beads. *AIChE Journal*, *54*(8), 2190–2197.

van der Zwan, E., Schroën, K., van Dijke, K., & Boom, R. (2006). Visualization of droplet break-up in pre-mix membrane emulsification using microfluidic devices. *Colloids and Surfaces A: Physicochemical and Engineering Aspects*, *277*(1–3), 223–229.
van Dijke, K., de Ruiter, R., Schroën, K., & Boom, R. (2010). The mechanism of droplet formation in microfluidic EDGE systems. *Soft Matter*, *6*(2), 321–330.
van Dijke, K. C., Schroën, K., van der Padt, A., & Boom, R. (2010). EDGE emulsification for food-grade dispersions. *Journal of Food Engineering*, *97*(3), 348–354.
Vladisavljević, G. T., Kobayashi, I., & Nakajima, M. (2008). Generation of highly uniform droplets using asymmetric microchannels fabricated on a single crystal silicon plate: Effect of emulsifier and oil types. *Powder Technology*, *183*(1), 37–45.
Vladisavljević, G. T., Shimizu, M., & Nakashima, T. (2004). Preparation of monodisperse multiple emulsions at high production rates by multi-stage premix membrane emulsification. *Journal of Membrane Science*, *244*(1–2), 97–106.
Vladisavljević, G. T., Shimizu, M., & Nakashima, T. (2006). Production of multiple emulsions for drug delivery systems by repeated SPG membrane homogenization: Influence of mean pore size, interfacial tension and continuous phase viscosity. *Journal of Membrane Science*, *284*(1–2), 373–383.
Weiss, J., & Muschiolik, G. (2007). Factors affecting the droplet size of water-in-oil emulsions (W/O) and the oil globule size in water-in-oil-in-water emulsions (W/O/W). *Journal of Dispersion Science and Technology*, *28*(5), 703–716.
Yafei, W., Tao, Z., & Gang, H. (2006). Structural evolution of polymer-stabilized double emulsions. *Langmuir*, *22*(1), 67–73.
Zhao, C. -X. (2013). Multiphase flow microfluidics for the production of single or multiple emulsions for drug delivery. *Advanced Drug Delivery Reviews*, *65*(11–12), 1420–1446.